INVITED PAPER Special Issue on Adaptive Signal Processing Technology in Antennas

High-Resolution Techniques in Signal Processing Antennas

Yasutaka OGAWA[†] *and* Nobuyoshi KIKUMA[††], *Members*

SUMMARY Signal processing antennas have been studied not only for interference suppression but also for high-resolution estimation of radio environment such as directions-of-arrival of incident signals. These two applications are based on the common technique, that is, null steering. This tutorial paper reviews the MUSIC algorithm which is one of the typical high-resolution techniques. Examining the eigenvector beam patterns, we demonstrate that the high-resolution capability is realized by steering nulls. The considerations will be useful for understanding the high-resolution techniques in the signal processing antennas. We then describe a modified version of MUSIC (Root MUSIC). We show the performance and robustness of the method. Furthermore, we introduce radar target identification and two-dimensional radar target imaging. These study fields are new applications of the signal processing antennas, to which a great deal of attention has been devoted recently.

key words: *null steering, superresolution technique, MUSIC algorithm, Root MUSIC, radar imaging*

1. Introduction

Signal processing antennas have different fields of application. One of them is suppressing interference signals by steering pattern nulls [1]–[8]. This feature is important for radio communications and radar systems. Another application is high-resolution estimation of radio environment. We can estimate arrival directions and polarizations of incident signals [9]–[17], and scattering behavior of radar targets [18]–[25]. This technique is closely related with modern spectral estimation [26]–[28], and reveals much higher resolution capabilities than the conventional Fourier transform methods such as the periodogram or the Blackman-Tukey estimator [28]. (The most fundamental method of bearing estimation is scanning a main beam of a phased array. This is equivalent to estimation of the periodogram [10]. The resolution is, however, limited by the aperture size, which is referred to as the Rayleigh limit.)

Many high-resolution techniques have been proposed and studied, for example, the Capon's method (minimum variance estimation) [29], the MUSIC algorithm [30], the maximum entropy method and several other versions of the linear prediction method [28]. The performance of the techniques has been reported [31]–[36]. The high-resolution bearing estimation is actually related with the null steering technique stated previously. Gabriel demonstrated that the linear prediction filter is identical in configuration to a sidelobe canceller, and that the Capon's method is realized by the adaptive null steering array with the directional gain constraint [9].

This tutorial paper is written on purpose to emphasize the relation between the high-resolution capability and null steering, and to introduce some recently developed techniques. First, we explain the MUSIC algorithm from the viewpoint of steering pattern nulls. The considerations will be useful for an intuitive understanding of MUSIC which is one of the typical estimation methods. We then introduce a more recent and robust method, a modified version of MUSIC (Root MUSIC [14]). Furthermore, we describe other applications of the signal processing antennas. Specifically, we consider radar target identification and two-dimensional radar imaging. These fields have been studied extensively for recent years.

2. MUSIC Algorithm

The MUSIC algorithm presented by Schmidt [30] relies on an eigenanalysis of a correlation matrix of incident signals. The basic idea had been proposed by Pisarenko [42] for estimating spectral lines from time series. The MUSIC algorithm differs from other typical methods in that it utilizes noise eigenvectors. Since Schmidt proposed the MUSIC algorithm, the performance has been compared with that of other techniques [31]–[33].

We assume that D narrow-band signals are incident on an N-element array antenna as shown in Fig. 1 ($N > D$). We also assume that any two of the signals are incoherent each other. We represent an analytic signal of ith signal at a reference point (origin) by $s_i(t)$ $(i = 1, 2, \cdots, D)$. Note that an analytic signal has a complex value. Readers who are unfamiliar with analytic signal notation are referred to the literature [7]. We express the "mode vector" of the ith signal as $\boldsymbol{v}(\theta_i)$, where θ_i denotes the arrival direction of the signal. $\boldsymbol{v}(\theta_i)$ is an N-dimensional column vector. Each component of $\boldsymbol{v}(\theta_i)$ represents the relative phase at each

Manuscript received July 8, 1995.

[†]The authors is with the Division of Electronics and Information Engineering, Faculty of Engineering, Hokkaido University, Sapporo-shi, 060 Japan.

[††]The author is with the Department of Electrical and Computer Engineering, Faculty of Engineering, Nagoya Institute of Technology, Nagoya-shi, 466 Japan.

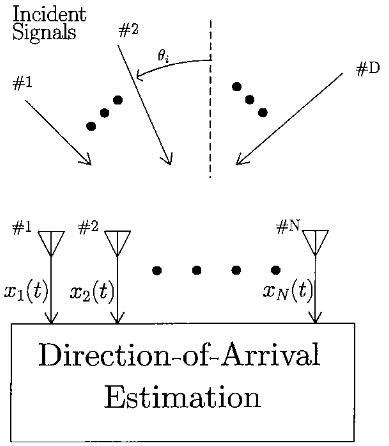

Fig. 1 Array antenna and signal environment.

antenna element. The relative phase depends on the location of the antenna element and arrival direction θ_i.

For a linear equispaced array as shown in Fig. 1, $\boldsymbol{v}(\theta_i)$ is expressed as

$$\boldsymbol{v}(\theta_i) = [\ 1\ e^{-j\frac{2\pi d}{\lambda}\sin\theta_i}\ e^{-j2\frac{2\pi d}{\lambda}\sin\theta_i} \cdots e^{-j(N-1)\frac{2\pi d}{\lambda}\sin\theta_i}\ ]^T \tag{1}$$

where λ and d denote the wavelength of the signal and the element spacing, respectively Also, ^{T} denotes transpose.

We introduce a D-dimensional column vector $\boldsymbol{s}(t)$ and an $N \times D$ matrix $\boldsymbol{A}$ as follows.

$$\boldsymbol{s}(t) = [s_1(t)\ s_2(t)\ \cdots\ s_D(t)]^T \tag{2}$$

$$\boldsymbol{A} = [\boldsymbol{v}(\theta_1)\ \boldsymbol{v}(\theta_2)\ \cdots\ \boldsymbol{v}(\theta_D)] \tag{3}$$

We represent the analytic signal of the output from the kth antenna element by $x_k(t)$ $(k = 1, 2, \cdots, N)$. $x_k(t)$ contains internal noise as well as the incident signals. We define an N-dimensional column vector $\boldsymbol{x}(t)$ as

$$\boldsymbol{x}(t) = [x_1(t)\ x_2(t)\ \cdots\ x_N(t)]^T. \tag{4}$$

Since the bandwidth of each signal is narrow, $\boldsymbol{x}(t)$ is given by

$$\boldsymbol{x}(t) = \boldsymbol{A}\boldsymbol{s}(t) + \boldsymbol{n}(t), \tag{5}$$

where $\boldsymbol{n}(t)$ is an N-dimensional column vector which denotes internal noise. The internal noises are assumed to be zero-mean complex Gaussian processes with variance (power) of σ^2, statistically independent of each other and the incident signals.

Here, we express the correlation matrix of $\boldsymbol{x}(t)$ as $\boldsymbol{R}_{xx}$. Thus, we have

$$\boldsymbol{R}_{xx} = <\boldsymbol{x}(t)\boldsymbol{x}(t)^H>, \tag{6}$$

where $< \cdot >$ and ^{H} denote ensemble average and complex conjugate transpose, respectively.

From Eqs. (5) and (6), $\boldsymbol{R}_{xx}$ is given by

$$\boldsymbol{R}_{xx} = \boldsymbol{A}\boldsymbol{S}\boldsymbol{A}^H + \sigma^2\boldsymbol{I}, \tag{7}$$

where

$$\boldsymbol{S} = <\boldsymbol{s}(t)\boldsymbol{s}(t)^H>. \tag{8}$$

Note that $\boldsymbol{I}$ denotes an $N \times N$ identity matrix.

Moreover, we represent the eigenvalues of $\boldsymbol{R}_{xx}$ by λ_m and the corresponding eigenvectors by $\boldsymbol{e}_m$ $(m = 1, 2, \cdots, N)$. We assume that $\lambda_1 \geqq \lambda_2 \geqq \cdots \geqq \lambda_N$.

Since the signals are incoherent, the matrix $\boldsymbol{S}$ is nonsingular, and we have the following expression [30].

$$\lambda_1 \geqq \lambda_2 \geqq \cdots \geqq \lambda_D > \lambda_{D+1} = \cdots = \lambda_N = \sigma^2 \tag{9}$$

D eigenvalues are larger than the noise power (σ^2), and the remaining $(N-D)$ eigenvalues are equal to the noise power. Thus, we can estimate the number (D) of the signals from the eigenvalue distribution.

The eigenvectors corresponding to the eigenvalues of σ^2 are referred to as the noise eigenvectors. The MUSIC algorithm uses the eigenstructure of the correlation matrix. The mode vectors of the signal are orthogonal to the noise subspace which is spanned by the noise eigenvectors. Then, we have

$$\boldsymbol{e}_m^H\ \boldsymbol{v}(\theta_i) = 0 \qquad m = D+1, D+2, \cdots, N \quad i = 1, 2, \cdots, D. \tag{10}$$

Here, we define the function $P_{music}(\theta)$ as

$$P_{music}(\theta) = \frac{\boldsymbol{v}(\theta)^H\boldsymbol{v}(\theta)}{\sum_{m=D+1}^{N} |\boldsymbol{e}_m^H\ \boldsymbol{v}(\theta)|^2}, \tag{11}$$

where $\boldsymbol{v}(\theta)$ denotes the continuum of all possible mode vectors. From Eqs. (10) and (11), it is seen that $P_{music}(\theta)$ has sharp peaks at θ_i $(i = 1, 2, \cdots, D)$. Thus, we may estimate the signal arrival directions by searching $P_{music}(\theta)$.

Now, we clarify the reason why the MUSIC algorithm has a high resolution capability. We consider the array antenna using the eigenvector $\boldsymbol{e}_m$ as shown in Fig. 2. e_{mk} $(k = 1, 2, \cdots, N)$ are the components of the eigenvector $\boldsymbol{e}_m$ and * denotes the complex conjugate. The analytic signal of the output is given by

$$y_m(t) = \boldsymbol{e}_m^H\ \boldsymbol{x}(t). \tag{12}$$

Furthermore, the antenna pattern of the array is expressed as

$$g_m(\theta) = |\boldsymbol{e}_m^H\ \boldsymbol{v}(\theta)|. \tag{13}$$

This is referred to as the eigenvector beam pattern [2]. Especially, the antenna pattern corresponding to the noise eigenvector is called the noise eigenvector beam pattern.

Now, we introduce the multiple beam antenna shown in Fig. 3. Each output $y_m(t)$ is given by Eq. (12). We define the output vector $\boldsymbol{y}(t)$ and an $N \times N$ matrix $\boldsymbol{Q}$ as

$$\boldsymbol{y}(t) = [y_1(t)\ y_2(t)\ \cdots\ y_N(t)]^T \tag{14}$$

$$\boldsymbol{Q} = \begin{bmatrix} \boldsymbol{e}_1^H \\ \boldsymbol{e}_2^H \\ \vdots \\ \boldsymbol{e}_N^H \end{bmatrix}. \tag{15}$$

Then, we have

$$\boldsymbol{y}(t) = \boldsymbol{Q}\boldsymbol{x}(t). \tag{16}$$

It is seen that the array pattern corresponding to the mth port is $g_m(\theta)$ which is given by Eq. (13). Since $\boldsymbol{R}_{xx}$ is an Hermitian matrix, $\boldsymbol{Q}$ is a unitary matrix. That is, $\boldsymbol{Q}\boldsymbol{Q}^H = \boldsymbol{Q}^H\boldsymbol{Q} = \boldsymbol{I}$ holds. From these results, it is seen that the array shown in Fig. 3 is the orthogonal multiple beam array.

From Eqs. (11) and (13), we obtain

$$P_{music}(\theta) = \frac{\boldsymbol{v}(\theta)^H \boldsymbol{v}(\theta)}{\sum_{m=D+1}^{N} \{g_m(\theta)\}^2}. \tag{17}$$

Also, from Eqs. (10) and (13),

$$g_m(\theta_i) = |\boldsymbol{e}_m^H\ \boldsymbol{v}(\theta_i)| = 0 \quad m = D+1, D+2, \cdots, N \quad i = 1, 2, \cdots, D \tag{18}$$

holds. The $(N-D)$ arrays which are determined by the noise eigenvectors form nulls on the signals. From Eq. (17), we see that $P_{music}(\theta)$ has peaks in the signal arrival directions θ_i $(i = 1 \sim D)$ in which the arrays having the patterns $g_m(\theta)$ $(m = D+1, D+2, \cdots, N)$ form the nulls. From these results, it may be said that the MUSIC algorithm estimates the signal arrival directions by detecting the nulls of noise eigenvector beam patterns in the multiple beam array. Since pattern nulls are in general sharp, the MUSIC algorithm achieves a great angular resolution beyond the Rayleigh limit determined by the array aperture. This is the reason for the high resolution capability of the MUSIC algorithm.

Now, we show the numerical results. A linear array of five elements having an equal spacing of half a wavelength has been considered. We assume that two uncorrelated signals are incident on the array from the angles θ_1 and θ_2 relative to broadside. We represent the signal-to-noise ratio of them by SNR_1 and SNR_2. Also, we assume that the exact (ensemble average) correlation matrix $\boldsymbol{R}_{xx}$ is available. The more snapshots of data we use, the more accurate correlation matrix we can estimate.

Eigenvector beam patterns are shown in Fig. 4. Since the array has five antenna elements, we have five eigenvector beam patterns. Figure 5 shows only the noise eigenvector beam patterns. It is seen that the nulls of the patterns are forced exactly in the signal arrival directions. This is consistent with the analytical considerations stated previously. Moreover, we see that the MUSIC algorithm successfully detects the signal arrival directions as shown in Fig. 6. ($\hat{D}$ denotes the estimated value of the number of signals.)

If the incident signals are coherent (magnitude of correlation coefficient = 1), the matrix $\boldsymbol{S}$ is singular, and the expressions (9) and (10) do not hold. In this case, we need spatial smoothing preprocessing before the MUSIC algorithm [37], [38].

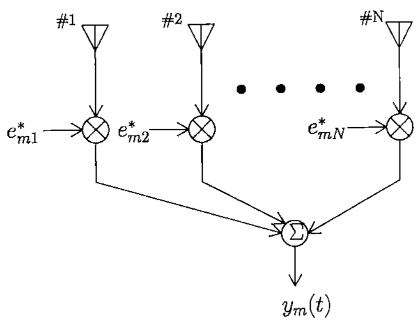

Fig. 2 Array antenna using eigenvector e_m.

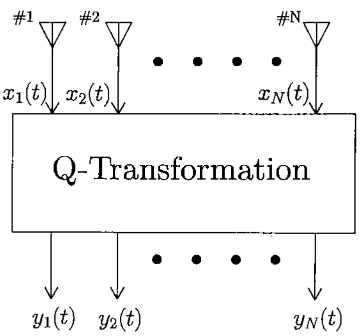

Fig. 3 Multiple beam array antenna using N eigenvectors.

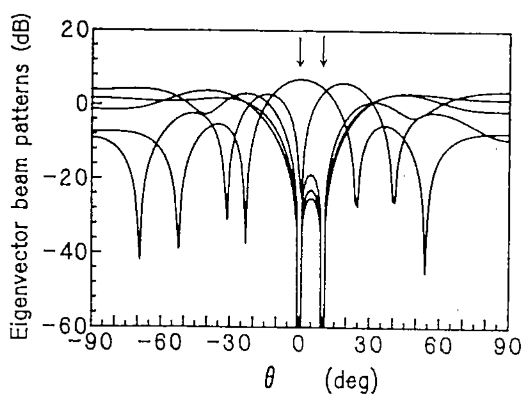

Fig. 4 Eigenvector beam patterns. The arrows indicate the signal arrival directions. $\theta_1 = 0°$, $\theta_2 = 10°$, $\mathrm{SNR}_1 = 30\,\mathrm{dB}$, $\mathrm{SNR}_2 = 20\,\mathrm{dB}$, $N = 5$.

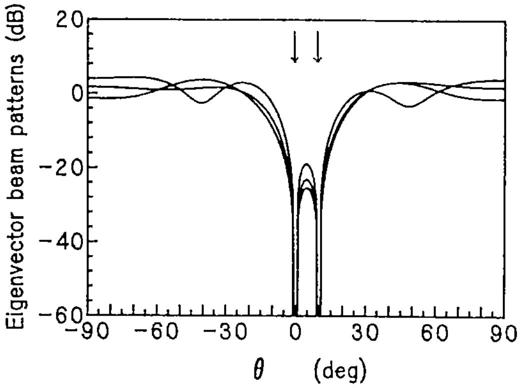

Fig. 5 Noise eigenvector beam patterns (1). The arrows indicate the signal arrival directions. $\theta_1 = 0°$, $\theta_2 = 10°$, $\mathrm{SNR}_1 = 30\,\mathrm{dB}$, $\mathrm{SNR}_2 = 20\,\mathrm{dB}$, $N = 5$.

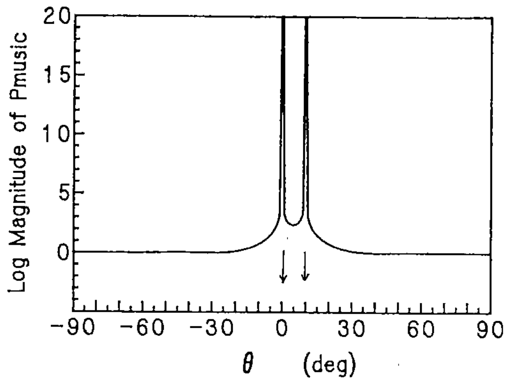

Fig. 6 Radio direction finding using the MUSIC algorithm (1). The arrows indicate the signal arrival directions. $\theta_1 = 0°$, $\theta_2 = 10°$, $\mathrm{SNR}_1 = 30\,\mathrm{dB}$, $\mathrm{SNR}_2 = 20\,\mathrm{dB}$, $N = 5$, $\hat{D} = 2$.

3. Root MUSIC Algorithm

Now, we describe Root MUSIC [14] which is a modified version of the MUSIC algorithm. In order to avoid confusion, the MUSIC algorithm stated previously is occasionally referred to as Spectral MUSIC.

When the SNR is low and/or snapshots of data are few, the estimation accuracy of the correlation matrix $\boldsymbol{R}_{xx}$ is poor, and the MUSIC algorithm degrades the performance as shown later. In these situations, Root MUSIC reveals better performance.

Although (Spectral) MUSIC is applicable to general array configurations, we need a linear equispaced array for Root MUSIC. We introduce an N-dimensional vector $\boldsymbol{z}$ given by

$$\boldsymbol{z} = [1\ z^{-1}\ z^{-2}\ \cdots\ z^{-(N-1)}]^T. \tag{19}$$

We define $S_m(z)$ using $\boldsymbol{z}$ and the noise eigenvector $\boldsymbol{e}_m$ as

$$S_m(z) = \boldsymbol{z}^T \boldsymbol{e}_m \qquad m = D+1, D+2, \cdots, N. \tag{20}$$

Also, the Root MUSIC polynomial Q(z) is defined as

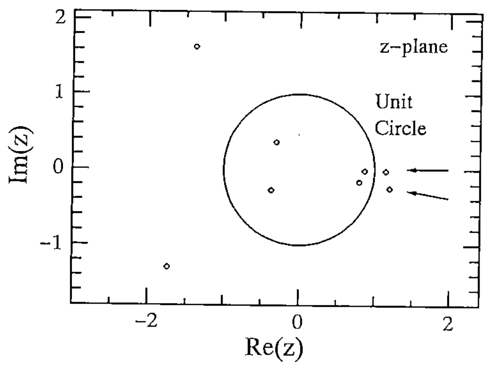

Fig. 7 Results of the Root MUSIC algorithm. The arrows correspond to the signal arrival directions. $\theta_1 = 0°$, $\theta_2 = 5°$, $\mathrm{SNR}_1 = \mathrm{SNR}_2 = 10\,\mathrm{dB}$, 50 snapshots, $N = 5$, $\hat{D} = 2$.

$$Q(z) = \sum_{m=D+1}^{N} S_m(z) S_m^*(1/z^*). \tag{21}$$

From Eqs. (1), (10) and (20), we see that

$$Q(z = e^{-j\frac{2\pi d}{\lambda}\sin\theta_i}) = 0 \tag{22}$$

holds. If $z = re^{j\phi}$ is one of the roots, then from Eq. (21), it is seen that $z = \frac{1}{r}e^{j\phi}$ is also the root of $Q(z) = 0$. Thus, we have root pairs with the same argument in the z-plane. We see that the roots on the unit circle ($r = 1$) are double roots.

Using Eqs. (20)–(22), we can formulate the Root MUSIC algorithm as follows.

1. We obtain the roots of the equation $Q(z) = 0$.
2. We have D double roots on the unit circle in the z-plane. These roots correspond to the actual incident signals.
3. From the arguments $(-\frac{2\pi d}{\lambda}\sin\theta_i)$ of these roots, we can estimate the arrival directions θ_i ($i = 1, 2, \cdots, D$).

The other roots which do not lie on the unit circle do not correspond to the signals, and are referred to as spurious roots. In an actual case where we have finite snapshots, the roots corresponding to the signals depart slightly from the unit circle. Discriminating the actual signal roots from the spurious roots is an important issue.

From Eqs. (1), (13) and (20), we see that $g_m(\theta) = |S_m(z = e^{-j\frac{2\pi d}{\lambda}\sin\theta})|$ holds. Thus, we can say that Spectral MUSIC treats the behavior of $S_m(z)$ and $Q(z)$ only on the unit circle in the z-plane. When SNR is lower and snapshots are fewer, the signal nulls depart from the unit circle. Occasionally, Spectral MUSIC fails to resolve signals, but Root MUSIC detects them.

Figure 7 shows the results of the Root MUSIC algorithm. The radio environment is harder than that in Figs. 4–6. Two signals have lower SNR, and are located closer. The correlation matrix is estimated using

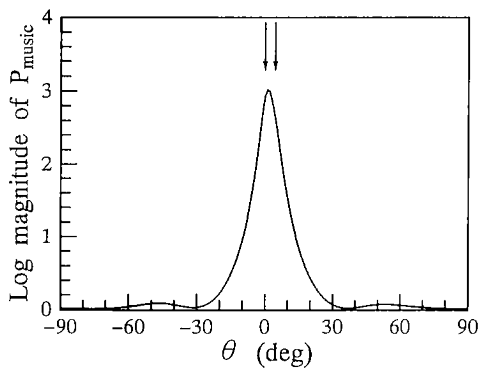

Fig. 8 Radio direction finding using the MUSIC algorithm (2). The arrows indicate the signal arrival directions. $\theta_1 = 0°$, $\theta_2 = 5°$, $\mathrm{SNR}_1 = \mathrm{SNR}_2 = 10\,\mathrm{dB}$, 50 snapshots, $N = 5$, $\hat{D} = 2$.

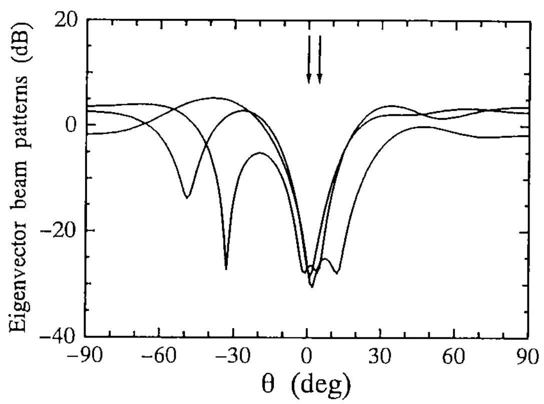

Fig. 9 Noise eigenvector beam patterns (2). The arrows indicate the signal arrival directions. $\theta_1 = 0°$, $\theta_2 = 5°$, $\mathrm{SNR}_1 = \mathrm{SNR}_2 = 10\,\mathrm{dB}$, 50 snapshots, $N = 5$.

50 snapshots of data. Although the roots corresponding to the signals depart from the unit circle, we can estimate the arrival directions $\hat{\theta}_1 = 0.4°$, $\hat{\theta}_2 = 3.8°$.

Figures 8 and 9 show the results of the Spectral MUSIC algorithm.

We cannot detect the two signals, and the nulls of the noise eigenvector beam patterns are not formed on these signals.

4. New Applications

We have described high-resolution radio direction finding. In this section, we present new applications of the signal processing antennas.

Scattering mechanism extraction is important for radar target identification. We obtain frequency-domain data using a stepped-frequency CW system. That is, we measure the amplitude and phase of the scattered wave at each frequency in the band. We can calculate the time-domain (down-range) profile by performing the inverse Fourier transform on the frequency-domain measurement [39]. However, the resolution of the time-domain response is limited by the available frequency band. Many targets are approximated as a set of discrete scattering centers at high frequency. Super-resolution techniques can be used to estimate the time-domain responses. Several study results have been reported [18]–[22].

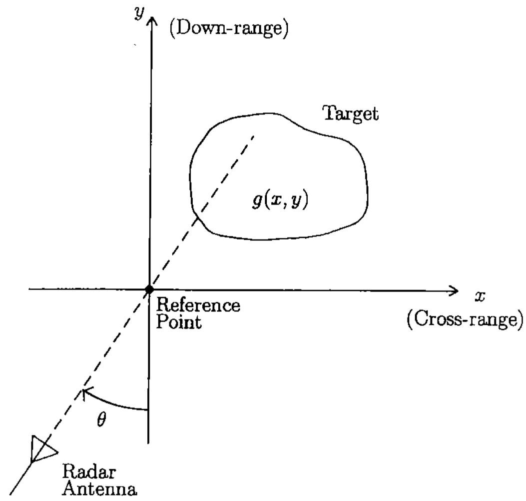

Fig. 10 Imaging geometry for a two-dimensional object.

Radar imaging has been studied extensively in recent years [40], [41]. We obtain an image of the target projected onto a cross-sectional plane. This technique is two-dimensional estimation. That is, we obtain down-range (time-domain) and cross-range (Doppler-domain) data.

Let a target, as shown in Fig. 10, have a two-dimensional distribution of scattering centers $g(x, y)$, denoted as the reflectivity density function.

The backscattered data at frequency f and aspect angle θ is given by

$$G(f, \theta) = \iint g(x, y) e^{-j\frac{4\pi f}{c}(x \sin\theta + y \cos\theta)} dx dy. \tag{23}$$

We can obtain $G(f, \theta)$ by measuring frequency-domain data at different aspect angles θ, if the variables f_x and f_y are defined as

$$f_x = \frac{2f}{c} \sin\theta,\ f_y = \frac{2f}{c} \cos\theta, \tag{24}$$

Eq. (23) is written as

$$G(f_x, f_y) = \iint g(x, y) e^{-j2\pi(f_x x + f_y y)} dx dy. \tag{25}$$

We see that $g(x, y)$ and $G(f_x, f_y)$ are a two-dimensional Fourier transform pair. $G(f_x, f_y)$ is the spatial spectrum, and f_x and f_y are spatial frequency. Thus, we can obtain the image of the object $g(x, y)$ by

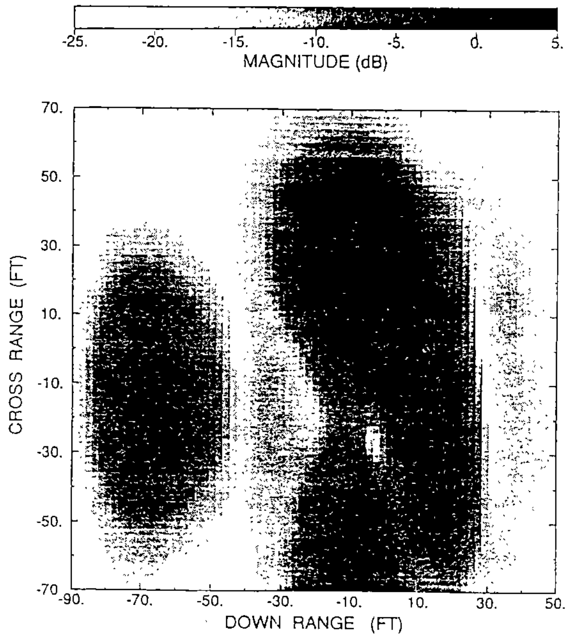

Fig. 11 Image of an aircraft using the two-dimensional inverse Fourier transform. $240\,\text{MHz} \leqq f \leqq 280\,\text{MHz}$, $-2^\circ \leqq \theta \leqq 2^\circ$.

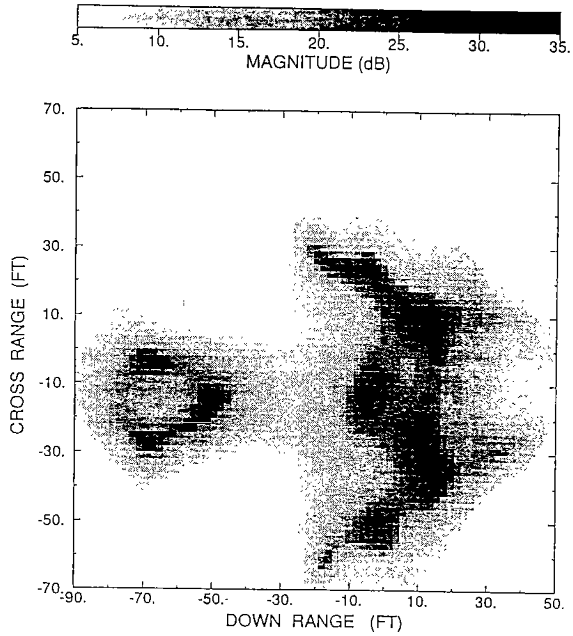

Fig. 12 Image of an aircraft using the two-dimensional linear prediction. $240\,\text{MHz} \leqq f \leqq 280\,\text{MHz}$, $-2^\circ \leqq \theta \leqq 2^\circ$.

performing the two-dimensional inverse Fourier transform of $G(f_x, f_y)$. This is the basic concept of a synthetic aperture radar (SAR) and an inverse synthetic aperture radar (ISAR) [40].

If the radar has a wide bandwidth and the target is observed over a large angular sector, we can achieve the high resolution. However, this is not possible in many applications. We assume that the target is well approximated as a set of discrete scattering centers. Then, we can improve the resolution using modern spectral estimation techniques [23]–[25].

Figure 11 shows an image of an in-flight aircraft (KC135) using the two-dimensional inverse Fourier transform [23]. The data were measured air-to-air by an airborne VHF/UHF radar. Figure 12 shows the image using the high-resolution technique (two-dimensional linear prediction [24]). From these figures, we see that the resolution is improved dramatically by the linear prediction method.

5. Conclusions

We have described the concept and important features of the MUSIC algorithm. Also, we have introduced the modified version of MUSIC (Root MUSIC). We may say that the estimation in the signal processing antennas is basically realized by steering nulls. A null is significantly sharper than a main beam. This is the reason why we can obtain the high-resolution capability.

The application of the signal processing antennas is not restricted to bearing estimation, but is expanded to the radar target identification and radar imaging. The high-resolution techniques are in a dynamic growing area. They may be applied to new other fields such as estimation of multipath propagation structure which will contribute to future digital mobile communications.

References

[1] B. Widrow, P.E. Mantey, L.J. Griffiths, and B.B. Goode, "Adaptive antenna systems," Proc. IEEE, vol.55, no.12, pp.2143–2159, Dec. 1967.
[2] W.F. Gabriel, "Adaptive arrays – an introduction," Proc. IEEE, vol.64, no.2, pp.239–272, Feb. 1976.
[3] IEEE Trans. Antennas Propagat., Special Issue on Adaptive Antennas, vol.AP-24, no.5, Sept. 1976.
[4] R.A. Monzingo and T.W. Miller, "Introduction to Adaptive Arrays," John Wiley & Sons, New York, 1980.
[5] J.E. Hudson, "Adaptive Array Principles," Peter Peregrinus Ltd., London 1981.
[6] B. Widrow and S.D. Stearns, "Adaptive Signal Processing," Prentice-Hall, Englewood Cliffs, 1985.
[7] R.T. Compton Jr., "Adaptive Antennas – Concepts and Performance," Prentice-Hall, Englewood Cliffs, 1988.
[8] E. Nicolau and D. Zaharia, "Adaptive Arrays," Elsevier, Amsterdam, 1989.
[9] W.F. Gabriel, "Spectral analysis and adaptive array supperresolution techniques," Proc. IEEE, vol.68, no.6, pp.654–666, June 1980.
[10] S. Haykin, ed., "Array Signal Processing," Prentice-Hall, Englewood Cliffs, 1985.
[11] IEEE Trans. Antennas Propagat., Special Issue on Adaptive Processing Antenna Systems, vol.AP-34, no.3, March 1986.
[12] J. Munier and G.Y. Delisle, "Spatial analysis in passive listening using adaptive techniques," Proc. IEEE, vol.75, no.11, pp.1458–1471, Nov. 1987.
[13] S. Haykin, ed., "Advances in Spectrum Analysis and Array Processing," I and II, Prentice-Hall, Englewood Cliffs,

1991.

[14] B.D. Rao and K.V.S. Hari, "Performance analysis of Root-Music," IEEE Trans. Acoust., Speech, Signal Processing, vol.37, no.12, pp.1939–1949, Dec. 1989.

[15] R. Roy and T. Kailath, "ESPRIT – estimation of signal parameters via rotational invariance techniques," IEEE Trans. Acoust., Speech, Signal Processing, vol.37, no.7, pp.984–995, July 1989.

[16] D.H. Johnson, "The application of spectral estimation methods to bearing estimation problems," Proc. IEEE, vol.70, no.9, pp.1018–1028, Sept. 1982.

[17] U. Nickel, "Angular superresolution with phased array radar: A review of algorithms and operational constraints," IEE Proc. F, Commun., Radar & Signal Process., vol.134, no.1, pp.53–59, Feb. 1987.

[18] E.K. Walton, "Comparison of Fourier and maximum entropy techniques for high-resolution scattering studies," Radio Sci., vol.22, no.3, pp.350–356, May–June 1987.

[19] M.P. Hurst and R. Mittra, "Scattering center studies via Prony's method," IEEE Trans. Antennas Propagat., vol.AP-35, no.8, pp.986–988, Aug. 1987.

[20] E.K. Walton, "Far-filed measurements and maximum entropy analysis of lossy material on a conducting plate," IEEE Trans. Antennas Propagat., vol.37, no.8, pp.1042–1047, Aug. 1989.

[21] R. Carriere and R.L. Moses, "High resolution radar target modeling using a modified Prony estimator," IEEE Trans. Antennas Propagat., vol.40, no.1, pp.13–18, Jan. 1992.

[22] A. Moghaddar, Y. Ogawa, and E.K. Walton, "Estimating the time-delay and frequency decay parameter of scattering components using a modified MUSIC algorithm," IEEE Trans. Antennas Propagat., vol.42, no.10, pp.1412–1418, Oct. 1994.

[23] E.K. Walton and I.J. Gupta, "Superresolution ISAR imaging techniques," Proc. 15th Meeting and Symp. Antenna Measurement Techniques Association, pp.277–281, Dallas, Texas, Oct. 1993.

[24] I.J. Gupta, "High resolution radar imaging using 2-D linear prediction," IEEE Trans. Antennas Propagat., vol.42, no.1, pp.31–37, Jan. 1994.

[25] J.W. Odendaal, E. Barnard, and C.W.I. Pistorious, "Two-dimensional superresolution radar imaging using the MUSIC algorithm," IEEE Trans. Antennas Propagat., vol.42, no.10, pp.1386–1391, Oct. 1994.

[26] S.M. Kay and S.L. Marple Jr., "Spectrum analysis – a modern perspective," Proc. IEEE, vol.69, no.11, pp.1380–1419, Nov. 1981.

[27] Proc. IEEE, Special Issue on Spectral Estimation, vol.70, no.9, Sept. 1982.

[28] S.M. Kay, "Modern Spectral Estimation: Theory and Application," Prentice-Hall, Englewood Cliffs, 1988.

[29] J. Capon, "High-resolution frequency-wavenumber spectrum analysis," Proc. IEEE, vol.57, no.8, pp.1408–1418, Aug. 1969.

[30] R.O. Schmidt, "Multiple emitter location and signal parameter estimation," IEEE Trans. Antennas Propagat., vol.AP-34, no.3, pp.276–280, March 1986.

[31] R.L. Johnson and G.E. Miner, "Comparison of superresolution algorithms for radio direction finding," IEEE Trans. Aerosp. Electron. Syst., vol.AES-22, no.4, pp.432–442, July 1986.

[32] M. Kaveh and A.J. Barabell, "The statistical performance of the MUSIC and the minimum-norm algorithms in resolving plane waves in noise," IEEE Trans. Acoust., Speech, Signal Processing, vol.ASSP-34, no.2, pp.331–341, April 1986.

[33] P. Stoica and A. Nehorai, "MUSIC, maximum likelihood, and Cramar-Rao bound," IEEE Trans. Acoust., Speech and Signal Processing, vol.37, no.5, pp.720–741, May 1989.

[34] U. Nickel, "Algebraic formulation of Kumaresan-Tufts superresolution method, showing relation to ME and MUSIC methods," IEE Proc. F, Commun., Radar & Signal Process., vol.135, no.1. pp.7–10, Feb. 1988.

[35] F. Li, R.V. Vaccaro, and D.W. Tufts, "Performance analysis of the state-space realization (TAM) and ESPRIT algorithms for DOA estimation," IEEE Trans. Antennas and Propagat., vol.39, no.3, pp.418–423, March 1991.

[36] H. Ye and R.D. DeGroat, "Maximum likehood DOA estimation and asymptotic Cramér-Rao bounds for additive unknown colored noise," IEEE Trans. Acoust., Speech Signal Processing, vol.43, no.4, pp.938–949, April 1995.

[37] T.J. Shan, M. Wax, and T. Kailath, "On spatial smoothing for direction-of-arrival estimation of coherent signals," IEEE Trans. Acoust., Speech, Signal Processing, vol.ASSP-33, no.4, pp.806–811, Aug. 1985.

[38] R.T. Williams, S. Prasad, A.K. Mahalanabis, and L.H. Sibul, "An improved spatial smoothing technique for bearing estimation in a multipath environment," IEEE Trans. Acoust., Speech, Signal Processing, vol.36, no.4, pp.425–432, April 1988.

[39] A. Dominek, L. Peters Jr., and W.D. Burnside, "A time domain technique for mechanism extraction," IEEE Trans. Antennas Propagat., vol.AP-35, no.3, pp.305–312, March 1987.

[40] D.L. Mensa, "High Resolution Radar Cross-Section Imaging," Artech House, Norwood, 1991.

[41] G. Dural and D.L. Moffatt, "ISAR imaging to identify basic scattering mechanisms," IEEE Trans. Antennas Propagat., vol.42, no.1, pp.99–110, Jan. 1994.

[42] V.F. Pisarenko, "The retrieval of harmonics from a covariance function," Geophys. J. Royal Astron. Soc., vol.33, pp.347–366, 1973.

Yasutaka Ogawa was born in Sapporo, Japan, on March 22, 1950. He received the B.S., M.S., and Ph.D. degrees from Hokkaido University, Sapporo, Japan, in 1973, 1975, and 1978, respectively. Since 1979, he has been with Hokkaido University, where he is currently a Professor of Electronics and Information Engineering. During 1992–1993, he was with ElectroScience Laboratory, the Ohio State University, U.S.A., as a Visiting Scholar, on leave from Hokkaido University. His special interests are in superresolution techniques, adaptive array antennas, and digital communication systems. Dr. Ogawa is a member of the IEEE and the Institute of Television Engineering of Japan.

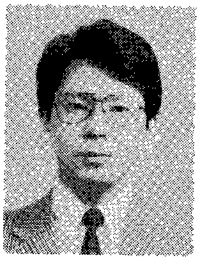

Nobuyoshi Kikuma was born in Ishikawa, Japan, on January 7, 1960. He received the B.S. degree in electronic engineering from Nagoya Institute of Technology, Japan, in 1982, and the M.S. and Ph.D. degrees in electrical engineering from Kyoto University, Japan in 1984 and 1987, respectively. From 1987 to 1988, he was a Research Associate at Kyoto University. In 1988 he joined Nagoya Institute of Technology, where he has been an Associate Professor since 1992. Currently, he is doing research on adaptive and signal processing array antennas, wireless communications and analysis of multipath propagation, and the related electromagnetic theory. Dr. Kikuma is a member of The Institute of Electrical and Electronics Engineers.